9950-674

(NASA-CR-169037) A STUDY PERTAINING TO A VERY LOW TEMPERATURE HYDROGEN MASER FEASIBILITY Final Report (Williams Coll.) 40 p HC A03/MF A01 CSCL 20E

N82-26654

Unclas G3/36 23507

FINAL REPORT

Contract 955441

with the

Jet Propulsion Lab

"A Study Pertaining to a Very Low Temperature Hydrogen Maser Feasibility"

Stuart B. Crampton
Principal Investigator
February 20, 1982

Williams College

I. LITERATURE STUDY

During the course of this work searches were made of the available literature relevant to this problem. References are given in this first section of this report in the context of a description of the recent work here and elsewhere.

Recent experiments here[1-4] and elsewhere[5-9] have demonstrated that ground state hydrogen atoms can be successfully stored in thermal equilibrium in low magnetic fields at liquid helium temperatures using containers coated with solid molecular hydrogen[1-6] or liquid helium.[7-9] The original motivation for this work was the theoretical prediction[10-12] that electron spin polarized hydrogen atoms $H\downarrow$ should undergo a phase transition to a superfluid gas at sufficiently high densities (10^{20} cm^{-3}) and low temperatures (0.2 K). Liquid helium surfaces have turned out to be by far the best surfaces for confining H at the very low temperatures needed to observe superfluidity in $H\downarrow$ gas, because of the very low binding energy of H to ^{4}He ($E_b \simeq 1.15$ K)[8] and ^{3}He ($E_b \simeq 0.42$ K).[9] Indeed, considerable progress in stabilizing $H\downarrow$ at 0.2 to 0.3 K has been achieved recently[13-15] using ^{4}He and ^{3}He storage surfaces.

In the earliest stages of this work it was realized by this Principal Investigator (PI) and his colleagues at MIT[16] and by others[17] that very low temperature H storage surfaces might make possible the development of very low temperature atomic hydrogen masers (VLTAHM) that would offer many advantages and new opportunities compared to the conventional room temperature hydrogen masers. These include (1) higher radiated power due to the higher beam intensities possible using low temperature techniques[4] and the much smaller electron spin flip cross section at low temperatures,[18-20] (2) lower cavity and amplifier noise temperatures, (3) increased stability

against mechanical creep at low temperatures, and (4) opportunities to extend H atom collision studies to low temperatures, where quantum effects and details of the interatomic potentials are much more important.

Considerable progress in the development of the VLTAHM has been achieved here and elsewhere. We have studied the adsorption of H on frozen H_2 surfaces at ambient temperatures from 3.2 K to 4.6 K.[3] (Ref. 3, which has been accepted for publication in Phys. Rev. B, is hereafter attached to this report as Appendix A.) We have used our findings to design a state-selected 6 K thermal H beam with potential of an improvement of beam intensity by a factor of 20 compared to room temperature beams.[4] (Ref. 4, which is the text of an invited paper delivered at the 3rd International Symposium on Frequency Standards and Metrology last fall and which will be published as it is in a supplement to J. Physique, is included with this report as Appendix B. Subsequent discussions of our work to date will refer to the apparatus description, the notation and the results presented in Appendices A and B.) Walter Hardy and his colleagues at the University of British Columbia (UBC) have studied the adsorption of H on liquid helium films at temperatures below 1 K[7-9] and have discussed possible applications of their results to the development of the VLTAHM.[21] Robert Vessot and his colleagues at the Smithsonian Astrophysical Observatory have constructed some apparatus for the observation of hydrogen maser oscillation down to liquid helium temperatures using CF_4 as a storage surface at first and perhaps some other surfaces later. As a result of conversations at the Frequency Standards Symposium we have begun close collaboration with Dr. Vessot's group.

Although the binding of H to liquid helium surfaces is weaker than can be expected from any other surface so far imagined, we believe that

the best prospects for an improved H maser frequency standard and spectrometer lie with the development of frozen neon surfaces to be used at about 10 K. The higher binding energy of H to neon will be more than compensated by the lower vapor pressure of neon and by the smaller electron spin exchange collision frequency shift cross section.[18-20] Our belief is based on the following work done here recently.

II. WORK PERFORMED

A. THEORY

Recently we have obtained an analytic solution for the distribution of times between collisions with the surface made by atoms having a thermal distribution of speeds stored within a spherical container. From this distribution of times we have obtained detailed numerical solutions for the resonance signal of atoms radiating at their free space frequency in between surface adsorptions on a spherical surface but relaxed and/or frequency shifted while adsorbed. Comparisons of these numerical results to predictions of the Central Limit Theorem (CLT) for such signals indicates that the CLT predictions are accurate up to surprisingly large perturbations while adsorbed. This theory permits the analysis of the frequency and radiative decay rate of the atoms in terms of the mean phase shift ϕ, the probability of relaxation ε, and the probability of not being adsorbed at all $(1 + \beta)^{-1}$, on an average trip across the storage container. Details of the theory are presented in Appendix A. When perturbations while adsorbed are small enough to allow the use of the CLT formulation, these results are easily extended to cw experiments and, in particular, to the case of an oscillating atomic hydrogen maser. These results are presented in Appendix C to this report.

B. ADSORPTION OF H ON FROZEN H_2 SURFACES, 3.2 K TO 4.6 K

We have developed techniques for making frozen H_2 surfaces for which the mean phase shift ϕ per trip to the surface is remarkably reproducible from one surface preparation to another. Moreover, the binding energies implied by the temperature dependence of ϕ agree with those predicted assuming smooth molecular crystal faces.[3] Due to the relatively high polarizability of H_2 per unit mass, the binding of H to H_2 is so strong that the frequency shifts and linewidths are rather large at temperatures where the vapor pressure of H_2 is low enough to allow H atoms into and across a storage bottle. However, the reproducibility of the H_2 surfaces near 4 K suggests that we should be able to make smooth and reproducible surfaces near 10 K of atomic neon, whose polarizability per unit mass is much less than either H_2 or helium. Details of the surface preparation techniques and other experimental details are presented in Appendix A.

C. LIQUID HELIUM TEMPERATURE, STATE-SELECTED H BEAM

The relatively high thermal accomodation coefficient and relatively low probability of recombination that we have observed for H atoms colliding with H_2 surfaces near 4 K have led us to design and construct a state-selected H beam with thermal speeds near 6 K. Details of the initial design and some preliminary results are presented in Appendix B. The experimental apparatus has since been rebuilt, and we expect soon to verify our design prediction[4] that state-selected beam intensities up to 20 times greater than those obtained with room temperature sources can be achieved with these techniques. In addition to having higher intensity, which may be useful for other applications in atomic spectroscopy and for the production of polarized proton beams and targets,[22] the beam is expected to be uniquely

free of non-H contamination. If maser action is to be achieved at low temperatures, a very clean state-selected H beam, or some other method of inverting the ground state level populations without introducing any contamination, is needed. Aside from other advantages of achieving maser action, it is helpful to have high signal-to-noise per unit density, since the limiting relaxation processes involve collisions between atoms while adsorbed on the surface in proportion to the gas phase density. In addition, we expect the relatively large population difference supplied by the state-selected beam to provide a diagnostic tool useful for unraveling the nature of the level population relaxation mechanisms, as described below.

D. LIQUID HELIUM SURFACES

What is in many ways the most promising very low temperature H storage surface is probably not compatible with the use of a state-selected beam or any "open" geometry. Recent results by Hardy and his colleagues at UBC indicate that the frequency shift of the H hyperfine transition frequency due to adsorption on ^{4}He and ^{3}He films is small only at temperatures where the vapor pressure of the He is very high.[8] For example, the deviation of the H hyperfine frequency from its free space value when stored using a liquid ^{4}He surface is given approximately by

$$f - f_0 = 8.5 \times 10^{-3}(T)^{-\frac{1}{2}}\,(A/V)e^{1.15/T} + 11.8 \times 10^{-18}n_{He} \qquad (1)$$

with n_{He} the saturated vapor pressure of He at temperature T and (A/V) the ratio of storage bottle surface area to volume. 1.15 K is the binding energy, assuming two-dimensional gas behavior of the adsorbed atoms. The first term is due to van der Waals perturbation of the hyperfine frequency

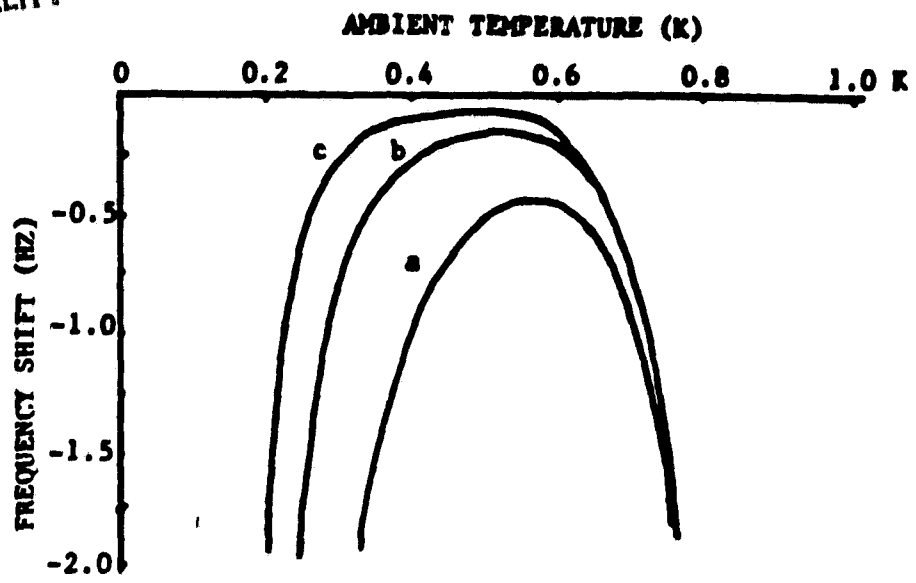

Fig. 1

Deviation of the *H* hyperfine frequency from its free space value for a liquid ^{4}He coated storage container at T

while adsorbed, and it dominates at the lowest temperatures. The second term is due to collisions with helium vapor atoms, and it dominates at higher temperatures. Eq. (1) is plotted in Fig. 1 for several choices of (A/V). a: $A/V = 4.3$, our guess at the geometry of the UBC experiments.[8] b: $A/V = 1.2$, the value for the 5 cm diameter used in our own experiments. c: $A/V = 0.4$, the value for 15 cm diameter spheres commonly used in room temperature atomic hydorgen masers and the value assumed by Hardy[21] in his recent analysis of the prosepcts for low temperature *H* masers using liquid helium surfaces. The frequency shift minimum just below 0.6 K moves downward in temperature and becomes lower and broader as (A/V) decreases. For the 15 cm diameter storage bottle the minimum frequency shift for ^{4}He is about 50 mHz at about 0.5 K, and the temperature coefficient of the (approximately quadratic) variation about the minimum is about 2.7 Hz K^{-2}.[21] The mimimum frequency shift on ^{3}He is about 36 mHz

and comes at about 0.2 K.[21] These frequency shifts are about the same size as those observed in room temperature hydrogen masers using Teflon coatings.[23] However, there are several difficulties to be overcome if these frequency shift minima are to be exploited for precision spectroscopy and frequency standard applications. The first is that the frequency shift minimum comes as a result of competition between two essentially different mechanisms, which may be affected differently by different kinds of perturbations and instabilities. For example, if there were to be a small temperature gradient across the storage bottle, the helium vapor density would tend to a value appropriate to a temperature below the average, while the surface adsorption times would average the temperature around the surface. The second is that the mean free path of H in helium vapor is very small at the temperature at which the frequency shift is a minimum. Hardy et al.[7] measure a diffusion cross section for H diffusing through ^{4}He near 1 K of $Q = 20(1) \times 10^{-16}$ cm^2. That corresponds to a mean free path of H in the helium vapor of roughly 0.04 cm at 0.6 K and roughly 0.5 cm at 0.5 K. It would be difficult to get a state-selected H beam into a storage bottle near 0.5 K. The storage time and details of the motional averaging of dc and rf magnetic fields would be very sensitive to helium vapor density and consequently to temperature and temperature gradients. The mean free path problem can be avoided by going to lower temperatures, but then the frequency shifts and temperature dependences of the frequency shifts become large. Finally, the electron spin exchange frequency shift cross section is predicted[18-20] to become large at temperatures below 1 K. For a pulsed resonance experiment at 0.5 K the ratio of spin exchange frequency shift to spin exchange contribution to the linewidth is predicted to be greater than one.[19]

Very interesting experiments have been done and remain to be done using liquid helium storage surfaces in a closed geometry like that of Hardy et al.[7-9] However, there are a number of reasons to choose instead to investigate neon surfaces at higher temperatures. Negative reasons include the difficulty of using a state-selected beam with helium surfaces and the very substantial cooling capacity required at 0.5 K in an open (for the state-selected beam) geometry in which there is a refluxing liquid helium film. Positive reasons are associated with the low polarizability of atomic neon per unit mass and the way in which cavity width and tuning can be used to measure and control the spin exchange frequency shift in an oscillating VLTAHM.[24]

III. RECOMMENDATIONS AND CONCLUSIONS

We conclude that state-selected atomic hydrogen masers are not only feasible but offer great promise for substantial improvements over room temperature atomic hydrogen masers. However, much further study is needed.

A. STATE-SELECTED ATOMIC HYDROGEN BEAM

The improved apparatus using a large bore hexapole has yet to be thoroughly evaluated. This evaluation should be carried out, and a comparison should be made to a shorter hexapole having a narrower bore, in order to check our numerical predictions about the tradeoffs between beam intensity and beam density depending on the bore.

B. MOLECULAR HYDROGEN STORAGE SURFACES ABOVE 5 K

Many questions remaining about the structure of these surfaces and the nature of hydrogen atom adsorption on them can be answered by extending the measurement upwards in temperature to 5.5 K or 6 K, where self-excited hydrogen maser oscillation should be easily obtainable using the state-selected beam.

C. ATOMIC NEON SURFACES NEAR 10 K

Atomic neon has less than half the polarizability of molecular hydrogen but ten times its mass. At low temperatures it forms a crystal similar in structure to the molecular hydrogen crystal structures and somewhat more compact, but the vapor pressure above solid neon is much less at the same temperature. Consequently, solid neon surfaces can be used to store hydrogen atoms at higher temperatures without being limited by collisions in the vapor. Because of the lower polarizability the binding to neon surfaces should be weak, and the van der Waals perturbation of the hyperfine frequency while adsorbed should also be weak compared to binding to molecular hydrogen. By roughly estimating the relevant parameters for hydrogen atoms adsorbed on neon surfaces, we have generated an equation similar to Eq. (1) but indicating a smaller and broader (with temperature) wall shift than the case of liquid helium surfaces. Atomic neon surfaces near 10 K should be studied carefully. The relevant parameters, which we have guessed by scaling, can be easily measured in an apparatus only very slightly modified from the apparatus we have been using.

IV. OVERALL CONCLUSION

This work and work done simultaneously elsewhere have shown that atomic hydrogen maser operation at liquid helium temperatures is feasible and that further developments are in order.

REFERENCES

[1]G. H. Zimmerman, III, Ph.D. Thesis, Harvard University, 1980 (unpublished); S. B. Crampton, G. H. Zimmerman, III, J. S. French, W. J. Hurlin, and J. J. Krupczak, Bull. Am. Phys. Soc. 25, 14 (1980); S. B. Crampton, S. P. Souza, W. J. Hurlin, and J. J. Krupczak, Bull. Am. Phys Soc. 25, 1149 (1980).

[2]S. B. Crampton, J. Phys. (Paris) Colloq. 41, C7-249 (1980).

[3]S. B. Crampton, J. J. Krupczak, and S. P. Souza, "Temperature Dependence of Hydrogen Atom Adsorption on Molecular Hydrogen Surfaces," submitted to Physical Review B and included in this proposal as Appendix A.

[4]Stuart B. Crampton, John J. Krupczak, and Steven P. Souza, "Progress of the State-Selected Beam Low Temperature Hydrogen Maser," text of an invited paper at the 3rd International Symposium on Frequency Standards and Metrology held at Aussois, France, in October 1981, included with this proposal as Appendix B.

[5]S. B. Crampton, T. J. Greytak, D. Kleppner, W. D. Phillips, D. A. Smith, and A. Weinrib, Phys. Rev. Lett. 42, 1039 (1979).

[6]W. N. Hardy, A. J. Berlinsky, and L. A. Whitehead, Phys. Rev. Lett. 42, 1042 (1979).

[7]W. N. Hardy, M. Morrow, R. Jochemsen, B. W. Statt, P. R. Kubik, R. M. Marsolais, and A. J. Berlinsky, Phys. Rev. Lett. 45, 453 (1981).

[8]M. Morrow, R. Jochemsen, A. J. Berlinsky, and W. N. Hardy, Phys. Rev. Lett. 46, 195 (1981) and Phys. Rev. Lett. 47, 455 (1981).

[9]R. Jochemsen, M. Morrow, A. J. Berlinsky, and W. N. Hardy, Phys. Rev. Lett. 47, 852 (1981).

[10]R. D. Etters, J. V. Dugan, and R. W. Palmer, J. Chem. Phys. 62, 313 (1975).

[11]M. D. Miller, L. H. Nosanow, and L. J. Parish, Phys. Rev. Lett. 35, 581 (1975).

[12]W. C. Stwalley and L. H. Nosanow, Phys. Rev. Lett. 36, 910 (1976).

[13]A. P. M. Matthey, J. T. M. Walraven, and I. F. Silvera, Phys. Rev. Lett. 46, 668 (1981) and G. H. van Yperen, A. P. M. Matthey, J. T. M. Walraven, and I. F. Silvera, Phys. Rev. Lett. 47, 800 (1981).

[14]R. W. Cline, T. J. Greytak, and D. Kleppner, Phys. Rev. Lett. 47, 1195 (1981).

[15]R. W. Cline, T. J. Greytak, and D. Kleppner, private communication, 1981.

[16]S. B. Crampton, W. D. Phillips, and D. Kleppner, Bull. Am. Phys. Soc. 23, 86 (1978).

[17]R. F. C. Vessot, E. M. Mattison, and E. L. Blumberg, Proceedings of the 33rd Annual Symposium on Frequency Control, P. 511 (Electronic Industries Association, 2001 Eye Street NW, Washington, D.C. 20006) (1979).

[18]A. C. Allison, Phys. Rev. A5, 2695 (1972) and A. C. Allison and F. J. Smith, Atomic Data 3, 317 (1971).

[19]A. J. Berlinsky and B. Shizgal, Can. J. Phys. 58, 881 (1980).

[20]Koyama and Baird, private communication, 1981.

[21]W. N. Hardy and M. Morrow, "Prospects for Low Temperature H Masers Using Liquid Helium Walls," invited paper at the 3rd International Symposium on Frequency Standards and Metrology held at Aussois, France, in October 1981.

[22]D. Kleppner, "Cold Hydrogen Techniques for Polarized Proton Production," to be published in the Proceedings of the Workshop on Polarized Proton Ion Sources, Ann Arbor 1981.

[23]S. B. Crampton, D. Kleppner, and N. F. Ramsey, Phys. Rev. Lett. 11, 338 (1963).

[24]S. B. Crampton, Phys. Rev. 158, 57 (1967).

B4-1 / BH 2122

APPENDIX A

Temperature Dependence of Hydrogen Atom Adsorption on Molecular-Hydrogen Surfaces

S. B. Crampton, J. J. Krupczak, and S. P. Souza

Department of Physics and Astronomy
Williams College
Williamstown, Massachusetts 01267

~~Received~~

(RECEIVED 3 1 AUGUST 1981)

~~ABSTRACT~~

The temperature dependence of the mean surface dwell time for hydrogen atoms adsorbed on polycrystalline molecular hydrogen surfaces has been measured over the temperature range 3.2 K to 4.6 K using magnetic resonance of the hydrogen atom ground state hyperfine transition. The mean surface dwell time is reproducible from one surface preparation to another and is exponential with inverse temperature with exponent 39.79(32) K. A detailed theory is presented of the magnetic resonance signal of a dilute gas subject to perturbations while adsorbed on the surface of its container.

PACS number : 68.10Jy

length of time adsorbed. Random dephasing as the atoms collide with the surface leads to resonance linewidths and frequency shifts which provide information about the adsorption process. Earlier results[4] suggested a temperature dependence of $\langle t_a \rangle$ much smaller than expected from the overall size of $\langle t_a \rangle$ at 4.2 K. We have since improved both the apparatus and the theoretical analysis of the line widths and shifts. In the present paper we report the detailed theory of the pulsed resonance experiment and results for the temperature dependence of $\langle t_a \rangle$. Some preliminary discussions of this work have appeared elsewhere.[6,7]

II. Apparatus

FIG. 1

Figure 1 is a schematic diagram of the apparatus. H atoms are produced in a rf discharge cooled by liquid nitrogen. Atoms emerging from a 2 mm diameter source orifice travel down about 20 cm of 11 mm ID pyrex tubing to a roughly spherical storage bottle with inner diameter about 5 cm. Everything below the source liquid nitrogen dewar is immersed in a liquid helium bath whose temperature is controlled by regulating the helium gas pressure over the bath. All interior surfaces below the source are covered by solid molecular hydrogen prepared by slowly freezing about 0.1 mole of H_2 as the cryostat is cooled.

The storage bottle is centered in a cylindrical microwave cavity[8] tuned to the 1420 MHz hydrogen atom ground state hyperfine transition

At temperatures above 4.2 K the signals give better fits to exponentially damped cosines having smaller $1/T_2$ and $\Delta\omega$. At temperatures of order 3.5 K and below the signals decay at rates approaching the collision rate, and they give less good fits to exponentially damped cosines, as

FIG. 3 illustrated by Fig. 3.

A. The Hydrogen Source

In the earliest stages[13] of this work H atoms were produced in a room temperature rf or dc discharge and piped down about 40 cm of 11 mm ID pyrex tubing to a 10 cm ID storage bottle under liquid helium, where they were detected by detecting the heat of recombination on a platinum wire. The flux of atoms reaching the storage bottle was insufficient for the observation of the hyperfine resonance. Subsequently, we determined that the discharges produced some impurity, presumed to be H_2O, that condensed out on the surfaces at liquid nitrogen temperatures and below but left residual vapor pressures at room temperature in a 1 liter system as high as several tens of microns after a few minutes of running the discharge at high power at microwave or rf frequencies. Cooling the discharge with liquid nitrogen was found to reduce the impurity production by several orders of magnitude. The present design provides liquid nitrogen cooling of a 180 MHz discharge and minimizes the area of surface below the discharge that is cold enough to condense H_2O but not cold enough to be covered by frozen H_2.

The rf power source is a high power tetrode vacuum tube (Amperex 7854) operated as a push-pull oscillator using a circuit described previously.[14]

which appears cloudy because of light scattering. The radiative decay rates $1/T_2$ and frequency shifts $\Delta\omega$ for such surfaces are from 10% to 20% higher than for smooth surfaces at the same temperature. Smooth surfaces are obtained either by annealing the initially rough surfaces or by forming the surfaces more slowly in the first place. Annealing is accomplished simply by warming the apparatus slowly until the majority of the solid H_2 has vaporized and then refreezing. Initially smooth surfaces are obtained by running the transfer tube down past the cavity (see Fig. 1), so that during the initial stages of the liquid helium transfer cold helium gas slowly cools the storage bottle surface to below the H_2 freezing point over a period of a few minutes. The properties of these slowly formed surfaces are unchanged by annealing. We have as yet no way to characterize the smoothness of our "smooth" surfaces on a microscopic level. They do not scatter light, and the radiative decay rates and frequency shifts of atoms colliding with them are reproducible from surface to surface and for a particular surface as recombined H_2 builds up on it during an experiment to within our 1% to 2% measurement errors at 4.2 K.

field amplitude over the storage bottle.

Following a suggestion by Greytak,[15] we write $P_{t_a}(\tau)$ as the sum over the number of trips that each atom has made across the storage bottle:

"sum over n"

$$P_{t_a}(\tau) = \sum_n P_n(\tau)\ p_n(t_a)\ , \qquad (2)$$

$P_n(\tau)$ is the probability that an atom has made just n trips across the bottle within time τ, and $p_n(t_a)$ is the probability that in just n trips an atom is adsorbed for total time t_a.

A. Adsorption Probability $p_n(t_a)$

For simplicity, we assume that the distribution of individual dwell times t_a is a simple exponential distribution function. If an atom were adsorbed once and only once on each trip all the way across the storage bottle, $p_n(t_a)$ would be simply the n-fold convolution of[16]

$$p_1(t_a) = 1/\langle t_s \rangle\ e^{-t_a/\langle t_s \rangle}\ , \qquad (3)$$

with $\langle t_s \rangle$ the mean sticking time per adsorption. The integral over t_a then gives

$$S(\tau) = e^{i\omega_o \tau} \sum_n P_n(\tau)\ z^n \qquad (4)$$

with

$$z = \frac{1}{1 - i(\delta\omega)\langle t_s \rangle}\ . \qquad (5)$$

Interactions that relax the oscillating atomic moments while the atoms are adsorbed, in addition to shifting their phases, are easily introduced to this model. If the probability per unit time "(lc) gamma" that an atom is relaxed while adsorbed is γ, Eq. (1) becomes

$$S(\tau) = e^{i\omega_o \tau} \int P_{t_a}(\tau)\, e^{i(\delta\omega)t_a}\, e^{-\gamma t_a}\, dt_a . \qquad (8)$$

Again, the result for the signal is Eq. (4) with z equal to

$$z = \frac{1 + \beta\epsilon - i\beta\phi}{1 + \epsilon(1+\beta) - i(1+\beta)\phi} . \qquad (9)$$

"(lc) epsilon" $\epsilon = \gamma\langle t_s\rangle s/(1-m) = \gamma \langle t_a\rangle$ is the probability of relaxing the oscillating moment on one trip across the storage bottle.

On this simple model the effects of surface adsorptions on the radiated signal are determined by only three parameters, ϕ, β, and ϵ. For example, if the probability that an atom makes just n trips across the storage bottle in time t were correctly described by a Poisson distribution with mean time between collisions equal to $\langle t_c\rangle$,

"n factorial" $$P_n(t) = \frac{1}{n!}\, (t/\langle t_c\rangle)^n\, e^{-(t/\langle t_c\rangle)} , \qquad (10)$$

Eq. (4) would sum to

$$S(\tau) = e^{-(1-z)\tau/\langle t_c\rangle} . \qquad (11)$$

The predicted signal would be an exponentially damped cosine with radiative decay rate $1/T_2$ and frequency shift $\Delta\omega$ given by

neglecting collisions between atoms. Maxwell-Boltzmann distribution of velocities to cross the storage bottle, For very large n, $P_n(\tau)$ is sharply peaked at $n = \tau/\langle t_c \rangle$, and the sum over n in Eq. (1) can be converted to an integral over n with limits extended to positive and negative infinity. The resulting signal is an exponentially damped cosine with radiative decay rate and frequency shift given by

$$i\,(\Delta\omega) - 1/T_2 = \log(z)\,[1 + \tfrac{1}{2}(\tfrac{9}{2\pi} - 1)\log(z)]\,/\langle t_c \rangle\,. \quad (15)$$

In the limit that z is very close to unity,

"approximately equal to"

$$\log(z) = \log[1-(1-z)] \approx -(1-z) = -\frac{\epsilon - i\,\phi}{1 + \epsilon(1+\beta) - i(1+\beta)\phi}\,, \quad (16)$$

to first order in $(1-z)$, and the central limit theorem approximation (CLTA) reduces to the Poisson distribution result. z is close to unity even for large ϵ or ϕ in the case when β is very much greater than unity, as in the case of the very low sticking coefficients observed by Morrow et. al.[17] for hydrogen atoms colliding with liquid ^{3}He and ^{4}He surfaces.

FIG. 4 Figure 4 displays the CLTA frequency shifts calculated for $\epsilon=0$ and a few small values of β, plotted as $(1+\beta)\,\Delta\omega\,\langle t_c \rangle$ against $(1+\beta)\phi$. $\Delta\omega$ increases linearly with ϕ for small ϕ, levels off at a value of order $[2(1+\beta)\langle t_c \rangle]^{-1}$ at $(1+\beta)\phi$ of order $\frac{\pi}{2}$, and then falls

FIG. 5 off to zero as ϕ becomes very large. Figure 5 displays the CLTA radiative decay rates calculated for $\epsilon=0$ and the same values of β, plotted as $(1+\beta)\,\frac{1}{T_2}\,\langle t_c \rangle$ against $(1+\beta)\phi$. $1/T_2$ increases

written in normalized time units as fractions of t_o.

"(uc) P sub naught"

The probability $P_0(\tau)$ of making zero collisions with the surface within time τ follows directly from h(t):

$$P_0(\tau) = 1 - \int_0^\tau h(t)\,dt = \mathrm{erf}\left(\frac{1}{\tau}\right) + (\pi)^{-\frac{1}{2}}\left[2\tau^3 - 3\tau - (2\tau^3 - \tau)\,e^{-\tau^{-2}}\right]. \quad (18)$$

"(lc) ρ ei"

Assuming diffuse desorption of atoms from the surface with probability proportional to cosψ of coming off at angle ψ with respect to the normal, the relative number of atoms that leave the surface between t and t+dt but have not yet hit the surface again a time T later is $(\pi/9)^{\frac{1}{2}}\,h(T)$. The relative number of atoms that hit the surface between t and t+dt, spend a time between t_a and t_a+dt_a adsorbed on the surface, and have not yet hit the surface again a time T later is $(\pi/9)^{\frac{1}{2}}\,h(t)\,dt\,p_1(t_a)\,dt_a\,h(T)$. The probability of making just one collision within the time τ is then (with $y=t+t_a$)

$$P_1(\tau) = (\pi/9)^{\frac{1}{2}} \int_0^\tau \int_0^y h(\tau-y)\,p_1(y-t)\,h(t)\,dt\,dy\,. \quad (19)$$

Using standard techniques,[16] we rewrite Eq. (19) as

$$P_1(\tau) = (36\pi)^{-\frac{1}{2}} \int_{-\infty}^{+\infty} F(k)\,Q(k)\,F(k)\,e^{-ik\tau}\,dk\,. \quad (20)$$

F(k) and Q(k) are the Fourier transforms of the distribution functions:

$$F(k) = \int_0^\infty h(t)\,e^{ikt}\,dt \quad (21)$$

$$Q(k) = \int_0^\infty p_1(t)\,e^{ikt}\,dt = \frac{1 - i\,k\,\beta\,\langle t_a\rangle}{1 - i\,k(1+\beta)\langle t_a\rangle}\,. \quad (22)$$

$\langle t_a \rangle$

$$S(\tau) = e^{i\omega_o\tau} \frac{1}{2\pi} \int_{-\infty}^{\infty} e^{-ik\tau} \left[\frac{i}{k} + (9/\pi)^{\frac{1}{2}} \frac{Q(1-G)^2(1-z)}{k^2\,(1-GQ)(1-GQz)} \right] dk \,, \quad (28)$$

In our experiments $\langle t_a \rangle$, which is the average time adsorbed per trip across the storage bottle, is less than $\langle t_c \rangle$ by a factor at least as small as 10^{-3} even at the lowest temperatures at which we have data. Consequently, Q(k) is not appreciably different from unity over the range of k contributing to the integrand of Eq. (28). We introduce little error by setting Q(k)=1, in order to obtain a somewhat simpler expression for S(τ).

$$S(\tau) = e^{i\omega_o\tau} \frac{1}{2\pi} \int_{-\infty}^{\infty} e^{-ik\tau} \left[\frac{i}{k} + (9/\pi)^{\frac{1}{2}} \frac{(1-G)\,(1-z)}{k^2\,(1 - G\,z)} \right] dk \,. \quad (29)$$

D. Approximate Behavior for Small Log(z)

An approximate solution for the signal S(τ) that is valid when z is close to unity can be obtained by expanding log[G(k)] for k near zero in the Gaussian form used as the starting point of the CLTA,[16]

$$GG(k) = e^{\,i(\pi/9)^{\frac{1}{2}} k \,-\, \pi f k^2/18} \,. \quad (30)$$

$f = 9/2\pi - 1$ is the ratio of the variance σ^2 to $\langle t_c \rangle^2$. The real and imaginary parts of GG(k) are compared in Fig. 7 to numerical solutions of Eq. (24) for the true G(k). GG(k) is a good approximation to G(k) out to about $k \approx \frac{1}{2}$ inverse normalized

FIG. 7

$\langle t_c \rangle = (\pi/9)^{1/2}$ in these normalized time units, so that Eq. (34) is identical to the Eq. (15) CLTA result. Assuming the Gaussian approximation to G(k), the signal for $z=1$ is an exponentially damped cosine with $\Delta\omega$ and $1/T_2$ correctly predicted by the CLTA. Small deviations from an exponentially damped cosine decay away in a time of order $\langle t_c \rangle$.

For small β or large ϕ or ϵ, so that z is not close to unity, the coefficient of the k_0 term in Eq. (33) no longer dominates the other coefficients and the $n=0$ decay rate becomes comparable to the $n \neq 0$ decay rates. The CLTA part of the signal is still the largest part at very long times, but at very long times the signal is essentially zero anyway. Even for times of order a few times $\langle t_c \rangle$, the contributions of a very large number of appreciable $n \neq 0$ terms produce large deviations from an exponentially damped cosine.

Equation (33) and the analysis following it provide a useful description of the signals to be expected in practice only to the extent that Eq. (29) is unaffected by the substitution of GG(k) for G(k). Detailed analysis indicates that GG(k) does give a good
FIG. 8 approximation to the integrand of Eq. (29). Figure 8 illustrates the agreement between the time independent parts of the Eq. (29) integrand, evaluated using GG(k) compared to using numerical G(k). For small log(z) the integral is dominated by resonant behavior at low k due to a nearby pole off the real axis. At low k GG(k) is a good approximation to G(k), and the substitution of GG(k) into Eq.
FIG. 9 (29) gives a good approximation to the signal. Figure 9 illustrates a similar comparison for a relatively large value of log(z). The resonant behavior has flattened out, leaving much larger relative

and theoretically, we expect from the study of Eq. (33) that the deviations from exponentially damped cosines should die out rapidly at the beginning of the signal. For example, we have calculated and fitted signals for $\epsilon=0$ and a variety of TD, β, and ϕ. If we take as the "parameterized" decay rates (PDR) and frequency shifts (PFS) the values fitted to exponentially damped cosines for TD about equal to $\langle t_c \rangle$, and if we take as the uncertainties the ranges of PDR and PFS as TD is varied from TD=0 to TD=$2\langle t_c \rangle$, we find that these PDR and PFS agree with the CLTA predictions to within the estimated uncertainties, which increase with $|\log(z)|$ roughly as $|\log(z)|^2$, reaching about 5% at $|\log(z)|=1$. We conclude that the CLTA should provide a remarkably good description of the signals in this type of experiment for parameters such that $|\log(z)|\ll 1$ even at quite short times after the start of the signal. For values of the parameters such that $|\log(z)|$ is not much less than one, as in the case of our own data at lower temperatures, the signal should still resemble an exponentially damped cosine, but care must be taken in the interpretation of fits of the signals to exponentially damped cosines.

IV. EXPERIMENTAL RESULTS

During each experiment the H_2 surface was prepared as described in Section II.B above, and data were taken at nine different temperatures between 3.2 K and 4.6 K. Each temperature was set by setting the vapor pressure over the bath using a pressure regulator. After waiting for ½ to 2½ hours for the temperature sensors to indicate that the apparatus had come to

exponential function of the time delay between π and π/2 pulses. Good fits were obtained to a combination of two exponentials having coefficients consistent with the hypothesis of a "fast rate" for mixing states within the F=1 upper hyperfine manifold and a "slow rate" for mixing the F=1 states
Fig 11 with the F=0 state. Figure 11 is a plot of the fast and slow rates against relative signal amplitude. At each temperature the slow rates were extrapolated to zero signal amplitude. The extrapolated slow rate was taken to be a rough estimate of $\epsilon/\langle t_c \rangle$, with error taken to be equal to the estimate itself. Note that the extrapolated rates are very low compared to the PDR, so that the large relative error in ε introduced little uncertainty to the final results over most of the temperature range.

At each temperature the experimental estimate of ε and guesses of ϕ and β were used to generate numerical simulations of the signal, using Eq. (29) and numerical G(k). An exponentially damped cosine was fitted to the simulated signal using points at the same time intervals Δ used to fit the experimental signals. Comparisons of the PDR and PFS fitted to the simulated signal and to the experimental signals were used to make new guesses of ϕ and β. The procedure was iterated until the experimental and theoretical PDR and PFS agreed to within the estimated experimental errors. CLTA estimates of the ϕ and β to produce particular PDR and PFS were used for the initial guesses, and only two or three iterations were generally required for convergence within errors.

Because of phase shifts in the electronics and small uncertainties in the pulse timing, there could be systematic errors in this procedure of matching the experimental and theoretical signals. The procedure was checked for one of the lowest temperature points by fitting the digitized experimental signal directly to a theoretical signal having variable

a straight line and the scatter of the results for β about a smooth curve are consistent with the reproducibility at 4.2 K.

$\phi(\frac{1}{T})$ gives good fits to exponentials with exponents 39.89(44) K and 39.94(48) K for the separate experiments displayed in Fig. 12. Combining the results of the two experiments, the mean adsorption time per trip across the storage bottle is

$$\langle t_a \rangle = 3.07(23) \times 10^{-5} \, (\delta\omega)^{-1} \, e^{[39.79(32)]/T} \text{ s.} \quad (35)$$

If we take $(\delta\omega)$ to be one-half its value for H trapped in a H_2 matrix,[19] or roughly 10^7 s^{-1}, then at 4.2 K $\langle t_a \rangle \approx 40$ ns. Extrapolating to 1 K would predict $\langle t_a \rangle \approx 1$ week.

C. Thermodynamic Binding Energies

The temperature dependence of $\langle t_a \rangle$ can be interpreted in terms of a binding energy by assuming simple thermodynamic models for the adsorbed phase. If the atoms are completely free to move laterally on the surface, so that they form a two-dimensional gas in equilibrium with the gas phase, simple thermodynamic arguments[20] predict that

$$\langle t_a \rangle = \frac{4\Lambda}{\langle v \rangle} e^{E/T} = \frac{4.80 \times 10^{-11}}{T} e^{E/T} \text{ s} \quad (36)$$

with Λ the Debroglie wavelength and $\langle v \rangle$ the mean thermal speed of the gas phase atoms at temperature T. E is the binding energy of the two-dimensional gas to the surface. Assuming again that $(\delta\omega)$ does not depend strongly on temperature in the restricted range 3.2 K to 4.6 K, Eq. (36) predicts that ϕ should vary as

$$\phi = \frac{4.80 \times 10^{-11} \, (\delta\omega)}{T} e^{E/T}. \quad (37)$$

thermodynamic arguments[20] predict that

$$\phi = \frac{1.45 \times 10^{-24} S_o (\delta\omega)}{T^2} e^{E/T} . \qquad (38)$$

S_o is the density of binding sites per unit area. Again, Eq. (38) fits the experimental data for $\phi(\frac{1}{T})$ as well but not significantly better than the alternative assumptions of simple exponential behavior or the two-dimensional gas. The fitted binding energy is E = 31.71(30) K, and the fitted $S_o (\delta\omega)$ = 2.56(18) x 10^{21} cm^{-2} s^{-1}. Again assuming $(\delta\omega) = 10^7$, $S_o = 2.6 \times 10^{14}$ cm^{-2}. S_o is of the order of the expected density of potential minima on a smooth but not perfectly planar molecular hydrogen crystal surface, and this fitted E is of the order of the expected binding to such a surface.[21]

The actual situation is undoubtedly more complicated than either of the extremes assumed by these simple thermodynamic models. What does seem significant about the analysis of our data is that, whatever the detailed nature of the binding of the atoms to the surface, it is consistent with the behavior to be expected for a uniform H_2 surface. In addition, our assumption that the binding is dominated by a single adsorption energy, so that the distribution of adsorption times is a simple exponential function of the time, appears to be justified.

The interpretation of the parameter β is complicated by its dependence on two other parameters, the sticking coefficient s and the multiple bounce coefficient m, about which we have no independent information. If we assume that m is independent of temperature because a purely geometrical factor, the temperature dependence of β can be interpreted in terms of models for s. In the models of Hollenbach and Salpeter[24] and Knowles and Suhl[25],

References

[1]W.C.Stwalley and L.H.Nosanow, Phys. Rev. Lett. 36, 910 (1976)

[2]J. T. M. Walraven, I. F. Silvera, and A. P. M. Matthey, Phys. Rev. Lett. 45, 449 (1980).

[3]R. W. Cline, D. A. Smith, T. J. Greytak, and D. Kleppner, Phys. Rev. Lett. 45, 2117 (1980).

[4]S. B. Crampton, T. J. Greytak, D. Kleppner, W. D. Phillips, D. A. Smith, and A. Weinrib, Phys. Rev. Lett. 42, 1039 (1979).

[5]W. N. Hardy, A. J. Berlinsky, and L. A Whitehead, Phys. Rev. Lett. 42, 1042 (1979).

[6]S. B. Crampton, J. Phys. (Paris) Colloq. 41, C7-249 (1980).

[7]G. H. Zimmermann, III, PhD Thesis, Harvard University, 1980 (unpublished); S. B. Crampton, G. H. Zimmermann, III, J. S. French, W. J. Hurlin and J. J. Krupczak, Bull. Am. Phys. Soc. 25, 14 (1980); S. B. Crampton, S. P. Souza, W. J. Hurlin and J. J. Krupczak, Bull. Am. Phys. Soc. 25, 1149 (1980).

[8]H. T. M. Wang, J. B. Lewis, and S. B. Crampton, Proceedings of the 33rd Annual Symposium on Frequency Control (Electronic Industries Association, 2001 Eye St. N.W., Washington DC 20006), p. 543 (1979).

[9]Lake Shore Cryotronics, Westerville, Ohio 43081, model DT-500P and CryoCal Inc., St. Paul, Minn. 55114, model CC 1000.

[10]MKS Instruments Inc., Burlington MA, model 220 BHS-2A2A-10K.

[11]International Microwave Corporation, model ACH-1420-80.

[12]IMSAI model 8080 with tape deck, disk drive and digital I/O. The computer was interfaced to this experiment by Dr. G. H. Zimmerman, III.

[13]D. Kleppner, T. J. Greytak, W. D. Phillips, D. A. Smith and A. Weinrib, Bull. Am. Phys. Soc. 23, 86 (1978).

[14]D. Kleppner, H. C. Berg, S. B. Crampton, R. F. C. Vessot, H. E. Peters, and J. Vanier, Phys. Rev. 138, A972 (1965).

[15]T. J. Greytak, (private communication, 1979).

[16]F. Reif, Statistical and Thermal Physics (McGraw Hill, N.Y., 1965), Ch. 1.

FIGURE CAPTIONS

Fig. 1 Schematic Diagram of the Apparatus. (A) H_2 inlet; (B) stainless steel liquid nitrogen dewar; (C) dissociator RF coil; (D) orifice; (E) quartz storage bottle; (F) microwave cavity; (G) coupling loop; (H) quartz cavity tuning rod; (I) cylindrical capacitor; (J) temperature sensors. The apparatus is immersed in liquid helium and surrounded by a solenoid and magnetic shields.

Fig. 2 1000 experimental signals taken at 4.2 K and averaged. Radiation by atoms in response to a $\pi/2$ stimulating pulse has been mixed down to audio frequency, digitized, and stored in 40 μs bins, after discarding the first 50 μs The first 7 of these data points, comprising the next 280 μs of the signal, have been discarded before fitting an exponentially damped cosine (solid curve) to the remaining data.

Fig. 3 1000 experimental signals taken at 3.4 K and averaged. The first 210 μs of the signal has been discarded before fitting the exponentially damped cosine depicted by the solid line.

Fig. 8 The real and imaginary parts of $\frac{i}{k} + (9/\pi)^{\frac{1}{2}} \frac{(1-G)(1-z)}{k^2 (1-Gz)}$ calculated for $\phi=0.2$, $\varepsilon=\beta=0$, and plotted against k. Separate curves plotted using the true G(k) and the Gaussian approximation GG(k) are indistinguishable on this scale. The real part (RE) is symmetric about a value of k where Gz=1, and the imaginary part (IM) is antisymmetric about that value of k.

Fig. 9 The real and imaginary parts of $\frac{i}{k} + (9/\pi)^{\frac{1}{2}} \frac{(1-G)(1-z)}{k^2 (1-Gz)}$ calculated for $\phi=1.6$, $\varepsilon=\beta=0$, plotted against k. In this case Gz=1 at a value of k where GG(k) is not a very good approximation to G(k). The curves RE(GG) and IM(GG) calculated using the Gaussian approximation to G(k) differ significantly from the curves RE(G) and IM(G) calculated using the true G(k). Note the changes of scale from Fig. 8 to Fig. 9.

Fig. 10 Numerical signal simulation using the true G(k) in Eq. (29) with $\phi=-.199$, $\beta=.555$ and $\varepsilon=.00078$. $\Delta\omega$ and $1/T_2$ from the exponentially damped cosine fitted to the signal beyond TD=96 μs match those fitted to an experimental signal at T=4.54 K.

B(-1.

Lab. Inga. (13)

CRAMPTON, et al.

BH 3122

ORIGINAL PAGE IS
OF POOR QUALITY

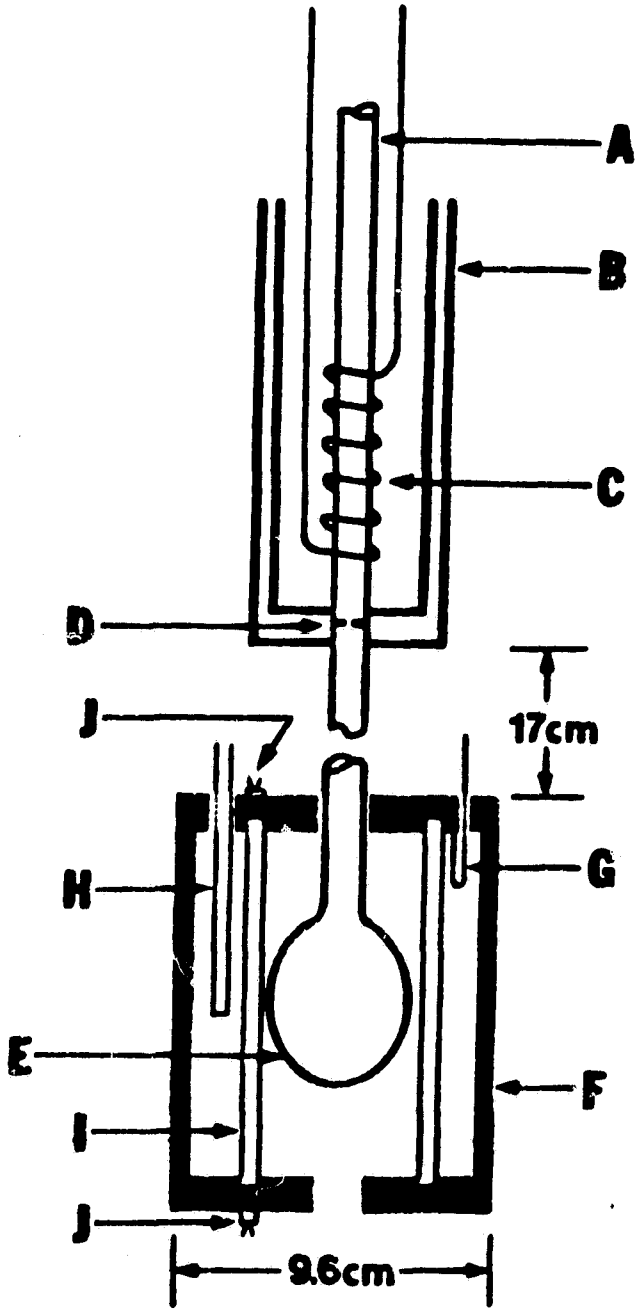

FIG. 1

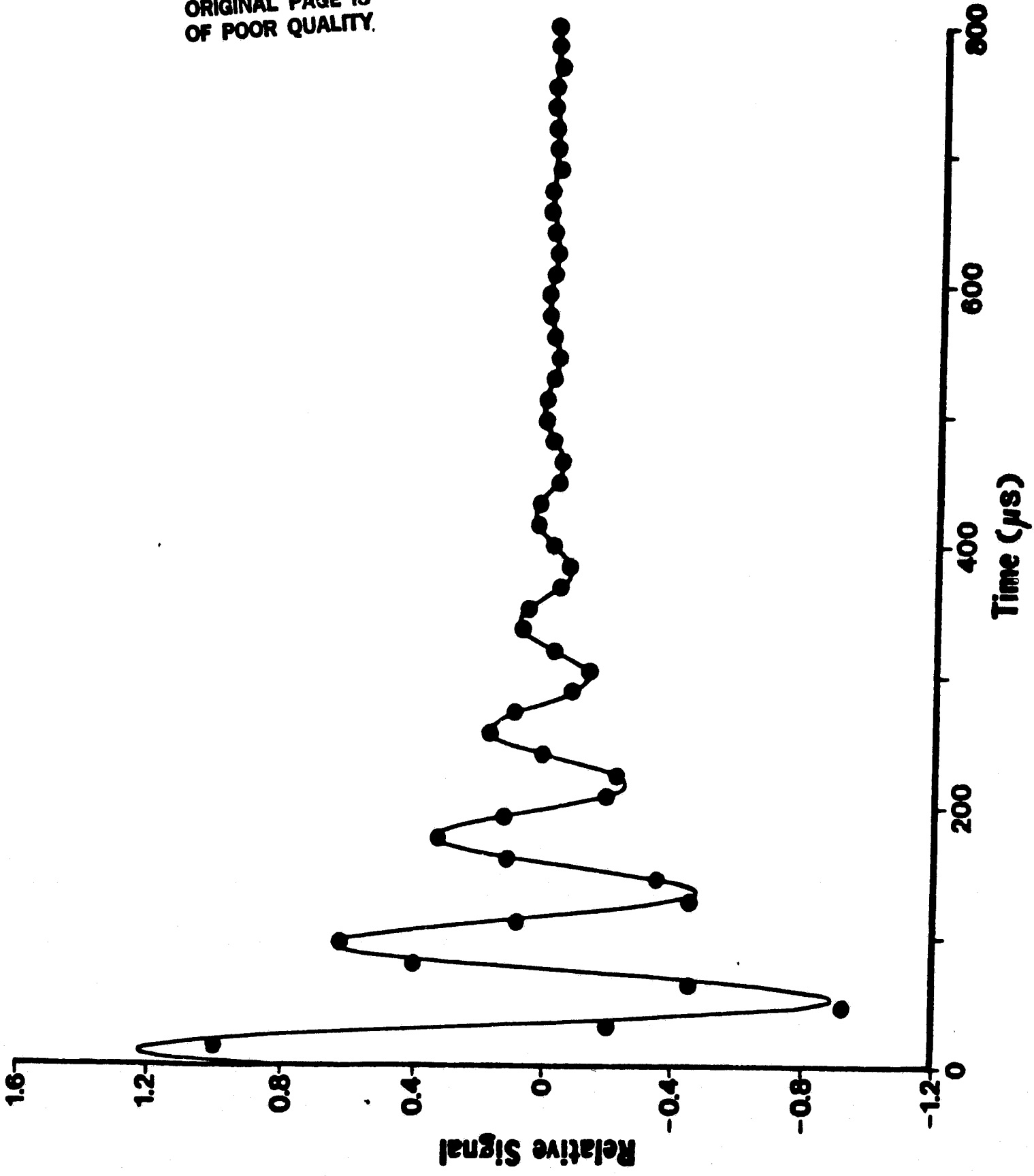

F16. 3

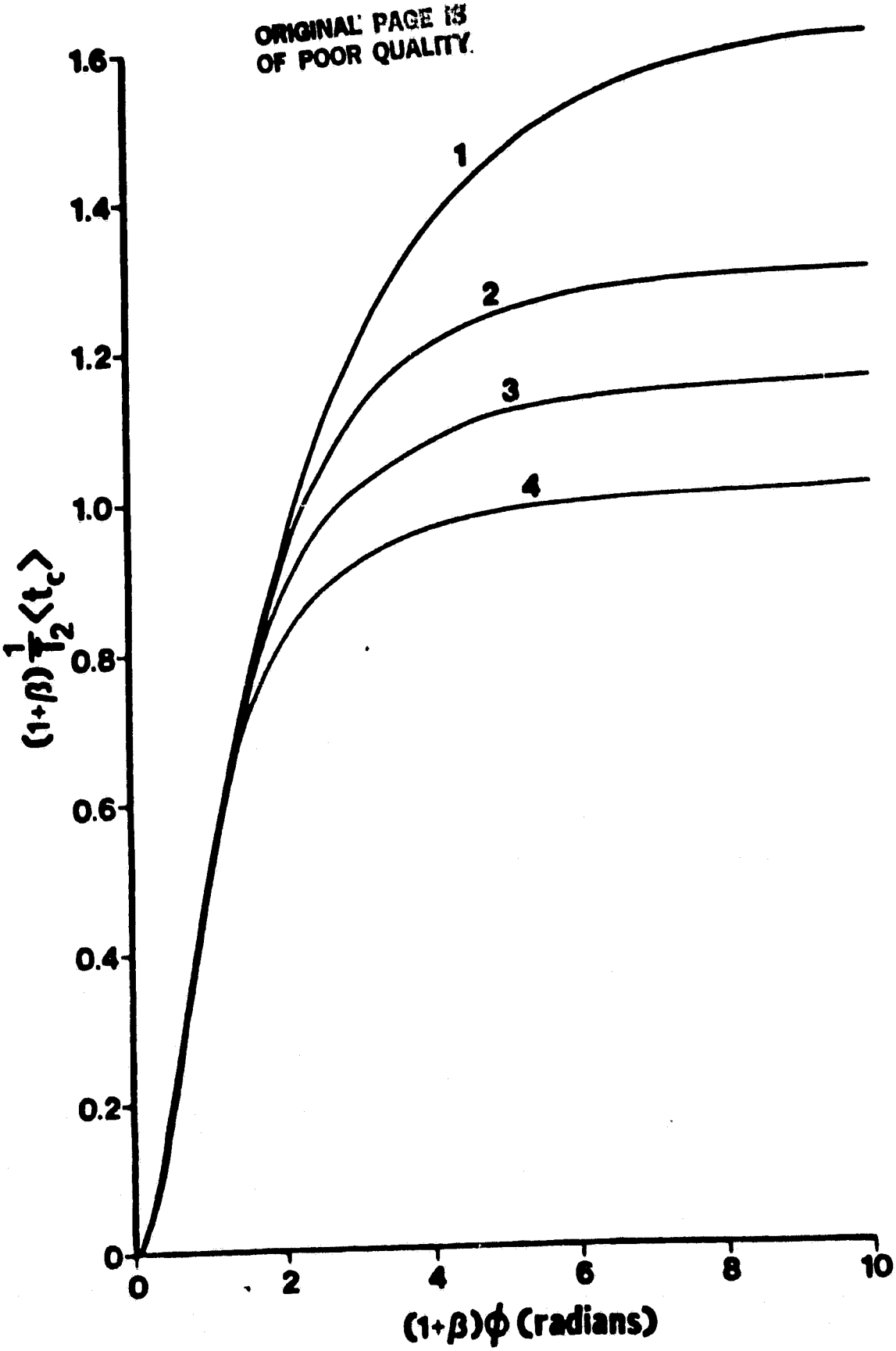

FIG. 5

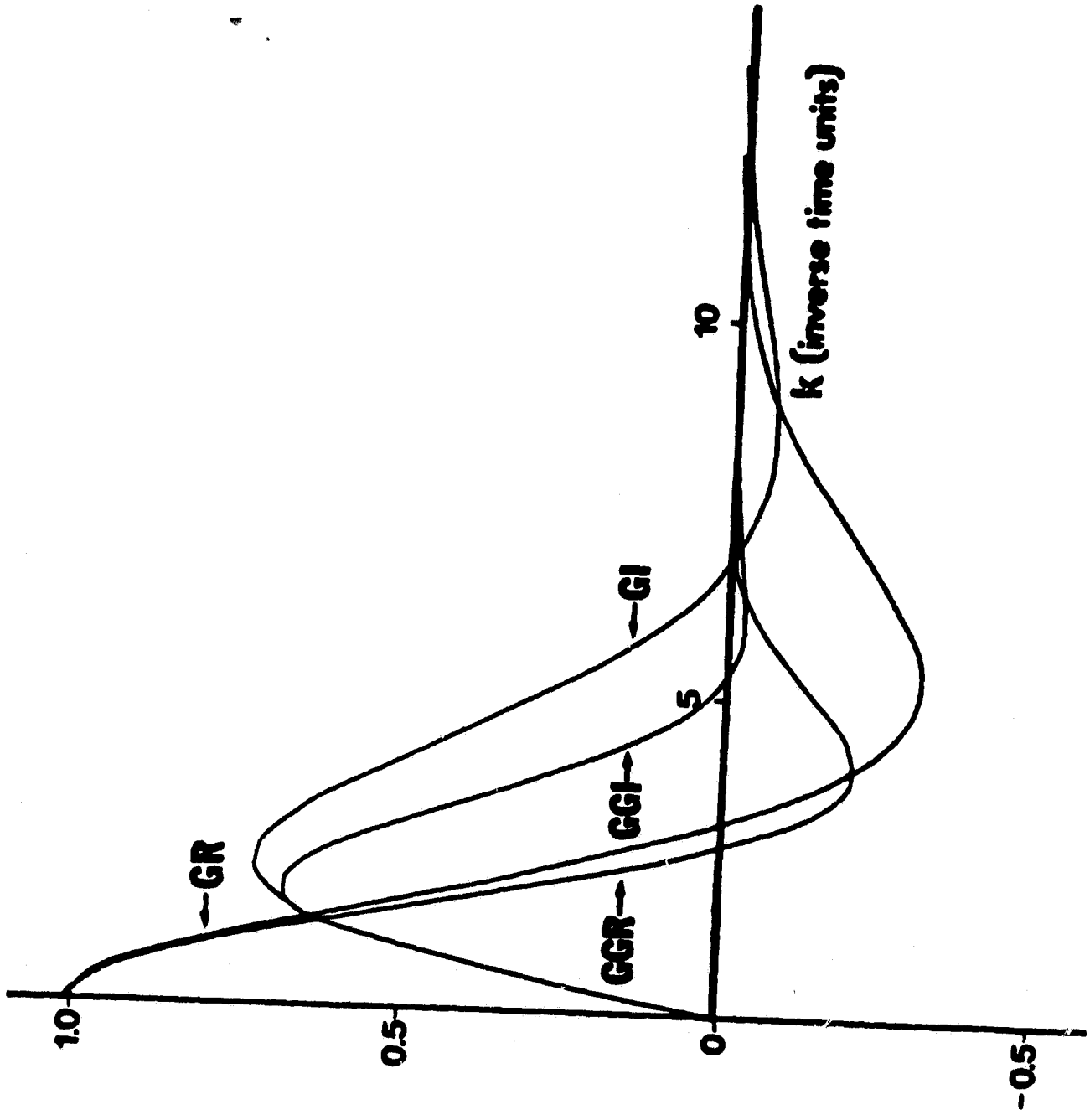

F16.7

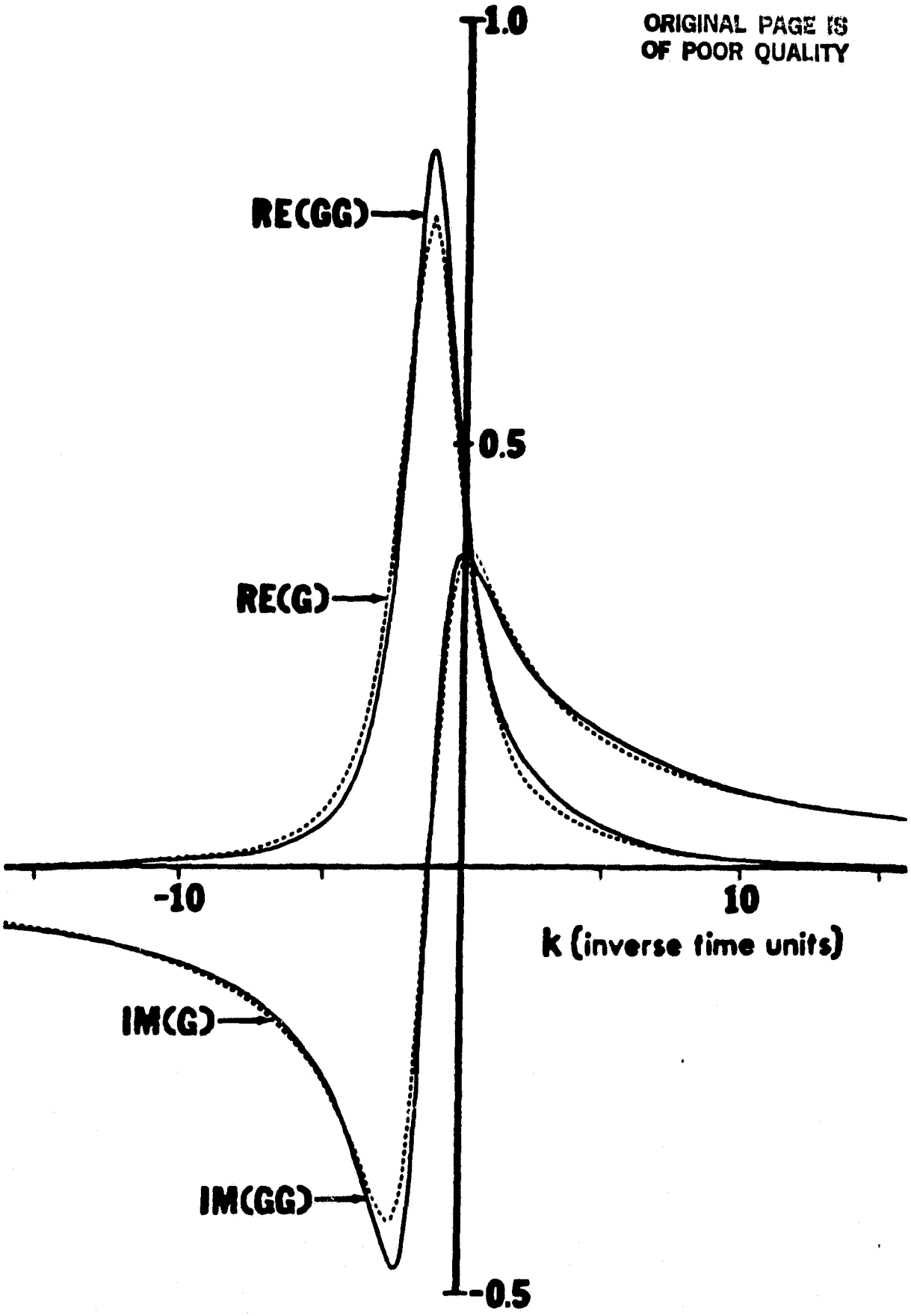

FIG. 9

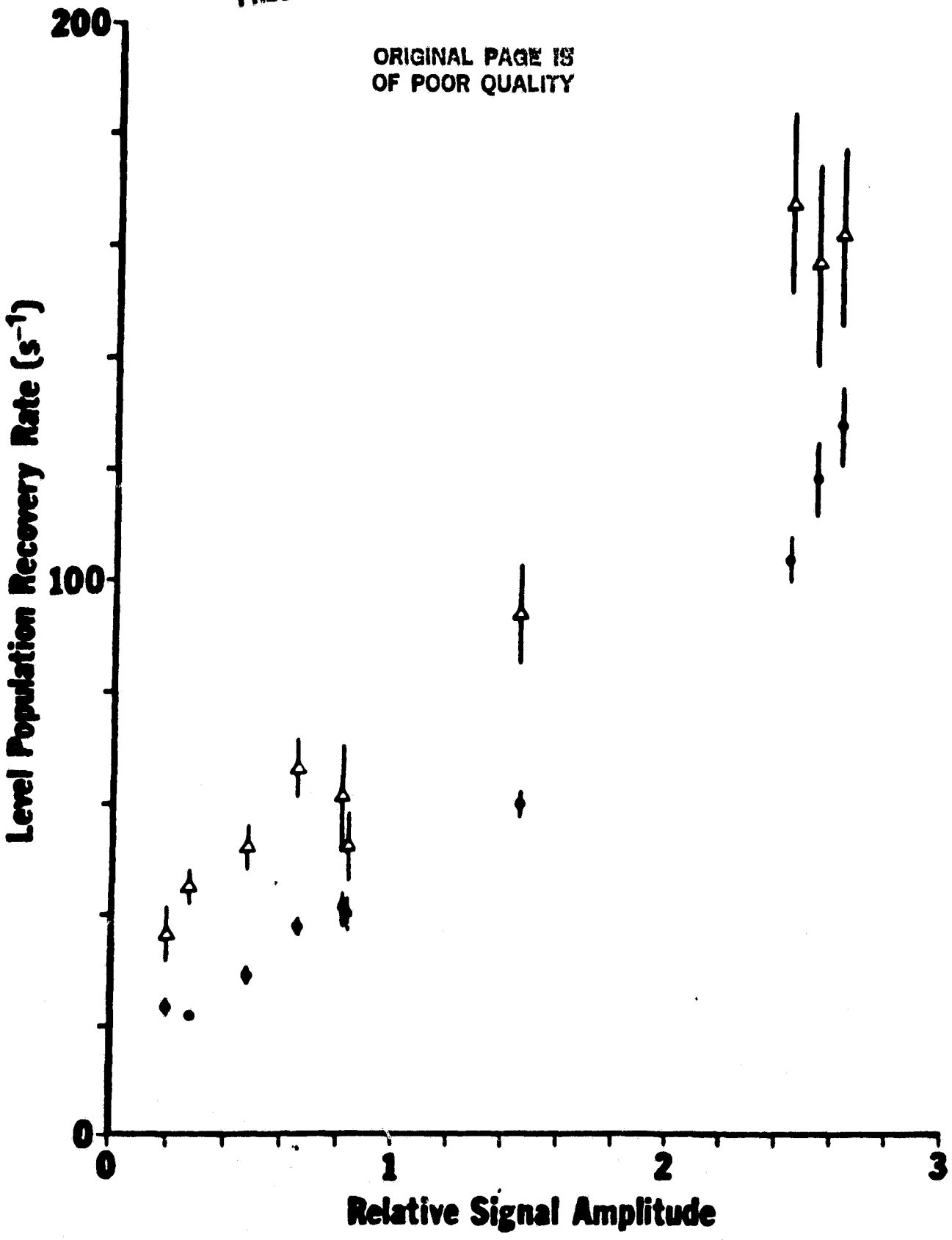

FIG. 11

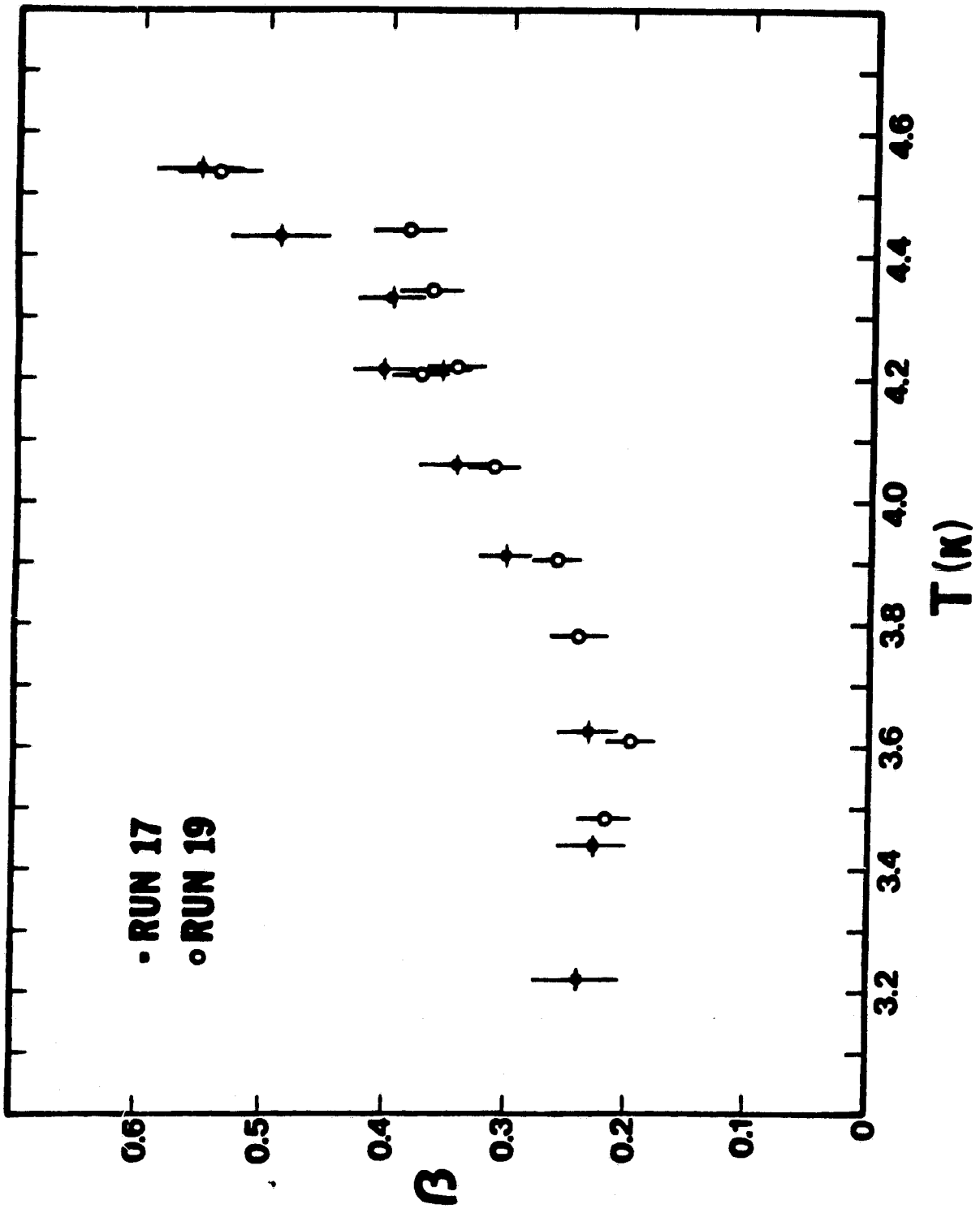

FIG. 13

APPENDIX B

Progress of the State-Selected Beam Low Temperature Hydrogen Maser

Stuart B. Crampton, John J. Krupczak and Steven P. Souza
Williams College, Williamstown, MA USA

Abstract.- We describe the source of a beam of liquid helium temperature state-selected hydrogen atoms to be used in the development of a very low temperature atomic hydrogen maser frequency standard. Recent experimental results which affect the design of such a beam are presented, and future experimental plans are outlined.

Introduction.- Recently published[1,2] and as yet unpublished studies by our laboratory of hydrogen atom (H) adsorption on polycrystalline molecular hydrogen (H_2) surfaces provide the basis for designing a source of a state-selected beam of polarized hydrogen atoms (H↑) thermalized at liquid helium temperatures. Attainable beam intensities and beam densities promise to be one or two orders of magnitude higher than those achieved with room temperature thermal H↑ beams. Any impurities other than He atoms should be effectively eliminated by cryopumping. Such beams should improve the signal-to-noise of low temperature studies of H,[1-5] and they may prove useful as sources and targets of polarized protons.

Adsorption of H on H_2.- Figure 1 illustrates the apparatus we have used to study the adsorption of H on H_2 at temperatures from 3.2 K to 4.6 K. H atoms are produced in a rf discharge cooled by liquid nitrogen. Atoms emerging from a 2 mm diameter source orifice travel down about 20 cm of 11 mm ID pyrex tubing to a 5 cm ID quartz storage bottle. Everything below the source liquid nitrogen dewar is immersed in a liquid helium bath whose temperature is controlled by regulating the helium gas pressure over the bath. All interior surfaces below the source are covered by solid molecular hydrogen frozen slowly from about 0.1 mole H_2 vapor as the cryostat is cooled. A short pulse of microwave radiation near the 1420 MHz H ground state hyperfine transition frequency induces the atoms to radiate a signal that decays in times of the order of milliseconds and whose frequency is shifted from the free space hyperfine frequency by amounts of the order of hundreds of Hz.

From the data we are able to extract the mean phase shift ϕ of the hyperfine frequency radiation phase per trip across the storage bottle and the mean probability α that an atom is adsorbed at least once while rattling around on the surface after a trip across the storage bottle. Figure 2

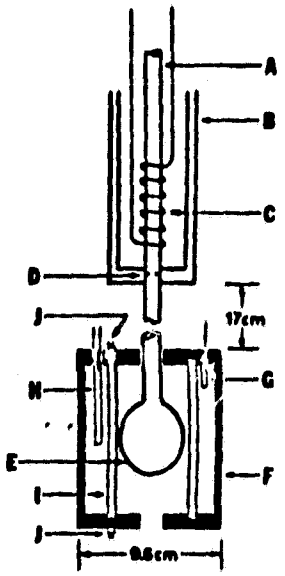

Fig. 1 : Schematic of the Adsorption Study Apparatus. (A) H_2 inlet; (B) stainless steel liquid nitrogen dewar; (C) dissociator rf coil; (D) orifice; (E) quartz storage bottle; (F) microwave cavity; (G) coupling loop; (H) quartz cavity tuning rod; (I) cylindrical capacitor; (J) temperature sensors.

circular baffles eliminate line of sight particles and radiation. Atoms in the upper two (F=1,m=1) and (F=1,m=0) ground state H hyperfine levels are focused by a hexapole magnet into a storage bottle coated with frozen H_2. They are detected by pulsing the hyperfine transition, as in the previous experiment.

The accomodator is cooled by conduction to the liquid helium bath through a 1 cm thick brass flange. A heater wound on the outside of the accomodator allows its temperature to be adjusted upwards. The hexapole magnet is 10 cm long and has a 1.3 cm diameter gap between pole pieces. The field at the pole pieces is about 2700 gauss. The magnet parameters have been chosen to optimally focus (F=1,m=0) atoms having thermal speeds at 7 K and starting as far off axis as possible.

The average number of surface collisions made by an atom passing through the accomodator is N_c=100, so that at T=4 K, γN_c=1 at n_H=2.5 x 10^{13} cm^{-3}. If the density at the accomodator were to saturate at about that value, the maximum flux from the accomodator would be about 4x10^{16} sec^{-1}. However, measurements of H_2 surface heating by H recombination in the storage bottle during the Fig. 1 experiment indicated that at optimum dissociator pressure and power about 4x10^{17} sec^{-1} atoms were delivered to the storage bottle at the end of an inlet tube in which atoms made 400 surface collisions on the average. At those high atom fluxes the temperature of the storage bottle surface was observed to rise by about 0.13 K. In the inlet tube above the storage bottle the density was much higher and the recombination heating per unit surface area that much greater. Evidently, the elevated H_2 surface temperature led to decreased γ and consequently to higher atom delivery than would have been expected if the inlet tube surface temperature had been only 4.2 K.

As the surface temperature rises, effects other than simply the decrease of γ come into play. From the measurements of Hardy et. al.[3] we know that the mean free path of H atoms in the saturated vapor of H_2 at 6 K is of the order of 0.2 mm. Unless the frozen H_2 above a few layers tightly bound to the substrate is pumped away to colder regions, the density of H_2 vapor above the H_2 surface will impede the H atoms and thereby increase the number of surface collisions they make in the accomodator. As γ decreases and the density of H that can be maintained above the surface increases, the mean free path of H in the H gas will fall below the characteristic dimensions of the accomodator and magnet. From the calculations of Allison and Smith[6] we estimate that the mean free path of H in H at n_H=10^{15} is of order 1 mm near 4 K. Not only will H-H scattering increase the number of surface collisions in the accomodator, but scattering in the magnet will interfere with state selection. If the H_2 density above the surface can be kept low by pumping away to colder regions, the useful accomodator H density will be limited by scattering in the H beam, as it is in the case of room temperature H beams, to about half the saturation density of room temperature beams. The low temperature source has the advantage of relatively efficient pumping by recombination on a warm, uncoated magnet and crypumping of the resultant H_2 by the magnet can walls, so that it should be possible to open up the source aperture more than is possible for room temperature sources. In addition, almost any impurity emerging from the source will be frozen out before reaching the storage bottle surface, an important consideration in frequency standard work.

Anticipated Magnet Performance.- If the accomodator exit aperture were very small compared to the magnet gap and the magnet gap were itself small enough that the magnetic moment of the (F=1,m=0) state were effectively saturated, the effective solid angle of the 7 K magnet would be about 300/7 that of a magnet for focusing 300 K atoms.[7] However, if some combination of the effects discussed above limits the accomodator density to some saturation value and if that saturation value itself depends on the number of surface collisions made in the accomodator, then it is useful to open up the accomodator exit aperture and choose magnet parameters so as to optimize focusing of off-axis atoms. We find that the magnet gap must be about three times the accomodator exit aperture diameter. For a large magnet gap the magnetic moment of the (F=1,m=0) state is far from saturation, and the usual methods for designing state-selecting magnets[7,8] break down appreciably. Consequently, we have resorted to Monte Carlo techniques in which the starting angles in front of the magnet are randomly selected and the trajectories are calculated numerically.

We find that the solid angle for focusing 7 K atoms from a small aperture through a circular hole 20 cm downstream having a diameter of the order of the 1.3

APPENDIX C

"Wall Shift" Saturation in Oscillating Hydrogen Masers At Low Temperatures

For low phase shift per wall collision there is no contribution to the linewidth relative to other effects, and the shift of the frequency of the oscillating maser is given simply by the phase shift per wall collision, divided by $\langle t_c \rangle$ = the mean time between wall collisions.

In the opposite limit of very high phase shift per wall collision, an atom is knocked so far out of phase by a wall collision that it no longer contributes to the oscillation after it has hit once. In that limit the lifetime is just the time to reach the wall once, and the frequency is not shifted from the free space frequency at all.

We expect then that as a function of the phase shift per wall collision, the wall shift will start off linearly with mean phase shift per wall collision but eventually peak out and fall to zero as the phase shift per wall collision gets very large. The linewidth should start off quadratically with phase shift per wall collision but saturate at a value of the order of $(\pi \langle t_c \rangle)^{-1}$.

An approximate description of the approach to saturation of the wall shift and linewidth can be obtained from our previous results for the case of pulsed resonance under conditions of large phase shift per wall collision. (See Crampton, Krupczak & Souza preprint entitled "Temperature Dependence of HYdrogen Atom Adsorption on Molecular Hydrogen Surfaces," 1981)

Starting from time $\tau=0$ the off-diagonal density matrix element describing the $\Delta m_F=0$ hyperfine transition $\rho_{42}(\tau)$ is given by what it would have been for zero wall collisions, multiplied by the $S(\tau)$ given in equation (1) of the preprint. If we assume that the aggregate linewidth is small compared to $\langle t_c \rangle^{-1}$, then we can differentiate $S(\tau)$ with respect to τ to get a contribution to the density matrix rate equations. If that assumption is not satisfied, the density matrix rate equation approach no longer is useful, but then the hydrogen maser is not very useful either.

$S(\tau)$ is a complicated function for which exact solutions are available only by numerical techniques. However, it is shown in the preprint that to a suprisingly good approximation the behavior of $S(\tau)$ is described by assuming a Gaussian distribution of collision times. In that case $S(\tau)$ is an exponentially damped cosine. Its time derivative is then just a (complex) constant times itself, and the contribution to the density matrix rate equations from wall collisions with large phase shift is a term

$$\frac{d}{dt}\rho_{42} = \frac{\log(z)}{\langle t_c \rangle}\left[1 + \tfrac{1}{2}\left(\frac{9}{2\pi} - 1\right)\log(z)\right]\rho_{42} \qquad \text{(I)}$$

with

$$z = \frac{1 + \beta\epsilon - i\beta\phi}{1 + (1+\beta) - i(1+\beta)\phi} \qquad \text{(II)}$$

ϕ is the mean phase shift per trip across the storage bottle; ϵ is the probability per trip across the bottle of a non-adiabatic relaxation of ρ_{42}; and $(1+\beta)^{-1}$ is the probability of being adsorbed at least once per trip across the bottle.

For low ϕ and $\epsilon=0$ the wall shift is

$$\delta\omega = \frac{\phi/\langle t_c \rangle}{1 + (1+\beta)^2\,\phi^2} \qquad \text{(III)}$$

to order ϕ^2. This equation is good only for very low ϕ; the approach to saturation is, however, given to a good approximation by equation (I), which is illustrated for the $\epsilon=0$ case in the preprint.